Université Scientifique et Médicale de Grenoble

INSTITUT DES SCIENCES NUCLÉAIRES
DE GRENOBLE

53, avenue des Martyrs - GRENOBLE

ISN 83.41
June 1983

HIGH-SPIN STATES IN THE TRANSITIONAL ODD-ODD NUCLEI ^{150}Eu AND ^{152}Tb

D. BARNEOUD[+], J.A. PINSTON[++], C. FOIN[+] and E. MONNAND[++]

[+]Institut des Sciences Nucléaires, Grenoble, France

[++]Centre d'Etudes Nucléaires, DSF/Chimie physique nucléaire, Grenoble, France

To be published in "Zeitschrift für Physik A"

Laboratoire associé à l'Institut National de Physique Nucleaire et de Physique des Particules.

HIGH SPIN STATES IN THE TRANSITIONAL ODD-ODD NUCLEI ^{150}Eu and ^{152}Tb

D. BARNEOUD+, J.A. PINSTON++, C. FOIN+ and E. MONNAND++.

+ Institut des Sciences Nucléaires (IN2P3), Grenoble, France.
++ Centre d'Etudes Nucléaires - DRF/Cnimie Physique Nucléaire, 85 X, 38041 Grenoble Cedex, France.

The (^{7}Li, 5n) and (^{11}B, 5n) reactions have been used to study the high-spin states in the two odd-odd nuclei ^{150}Eu and ^{152}Tb. Three decoupled bands have been evidenced in each nucleus belonging to the same configurations $[f\ \frac{7}{2}]_n\ [h\ \frac{11}{2}]_p$, $[h\ \frac{9}{2}]_n\ [h\ \frac{11}{2}]_p$ and $[i\ \frac{13}{2}]_n\ [h\ \frac{11}{2}]_p$. The latter oneis well developped and improves our knowledge of this system between the spherical and deformed region. The analysis of the collective moment of inertia and transition ratios strongly suggests an increase of the deformation when the rotational frequency increases in these two transitional nuclei ^{150}Eu and ^{152}Tb.

1. - INTRODUCTION -

During the last few years informations have been obtained on the band structure of the odd-odd nuclei in the deformed rare hearth region. Up to now the high-spin states have been studied in eight odd-odd nuclei : ^{152}Eu [1], ^{154,156}Tb [2], ^{156,158,160,162}Ho [3,4,5] and ^{158}Tm [6].

The common feature in all these nuclei is the presence of the decoupled $[i\frac{13}{2}]_n$ $[h\frac{11}{2}]_p$ band always strongly fed in the heavy ion reactions. It was shown [1,2] that the $[i\frac{13}{2}]_n$ $[h\frac{11}{2}]_p$ configuration carries an aligned angular momentum comparable with the value measured in the S-band of the neighbouring even-even nuclei, which fully explains the strong feeding of this band and the simplicity of the level schemes. Then the odd-odd nuclei are very certainly the most powerful systems to study the behaviour of two quasiparticles strongly coupled to a deformed core in rotation. Comparatively the considered system in odd-odd nuclei is more interesting than the S band. As a matter of fact the low frequency rotational states can be fed in the $[i\frac{13}{2}]_n$ $[h\frac{11}{2}]_p$ band while the levels reached in the S-band are mainly above the backbending frequency and moreover the states corresponding to the two different signatures $\alpha = 0$ (even spin) and $\alpha = 1$ (odd spin) are present in the $[i\frac{13}{2}]_n$ $[h\frac{11}{2}]_p$ band, while only the even spins are allowed by the Fermi-principle in the S-band.

On the other hand the $[i\frac{13}{2}]_n$ $[h\frac{11}{2}]_p$ configuration has also been identified in the ^{148,150}Tb spherical nuclei [7,8].

The main aim of the present investigation is to extend our knowledge of the odd-odd nuclei in the transitional region and for this purpose we have studied the N = 87 isotones ^{150}Eu and ^{152}Tb.

2. EXPERIMENTAL PROCEDURE -

The final nuclei ^{150}Eu and ^{152}Tb were produced respectively by the ^{146}Nd (^{7}Li,5n) and ^{146}Nd (^{11}B, 5n) reactions. Targets of Nd_2O_3 powder (4 mg cm^{-2}), enriched to 90% in ^{148}Nd and ^{146}Nd, were bombarded with the external ^{7}Li and ^{11}B beams from the Grenoble isochronous cyclotron. The γ-rays were detected with various high-resolution Ge(Li) or hyperpure-Ge detectors : a 3.3 cm^3 planar detector and large volume coaxial detectors.

The beam energy was chosen by comparison with the already known ^{150}Nd(^{7}Li,5n) [1] and ^{148,150}Nd (^{11}B,5n) [2] reactions and corrected for Q-value differences. By this procedure an energy of 50 MeV has been found for the ^{7}Li-beam and 66 MeV for the ^{11}B-beam. The analysis of the singles γ-spectra shows that the wanted ^{146}Nd (^{7}Li, 5n) ^{150}Eu and the ^{146}Nd (^{11}B,5n) ^{152}Tb reactions are the most prominent at these so determined energies (see Table 1). The relative reaction cross sections were determined from the delayed γ-decay of the 45 ns and 4.2 mn isomeric states in ^{150}Eu [9] and ^{152}Tb [10] respectively and from the prompt γ-emission of ^{149,151}Eu [11] ^{151,153}Tb [12,13], ^{150}Sm and ^{152}Gd [14] ; all these final nuclei were well known from other reactions. Although the excitation functions were not studied in this work we can conclude that the most prominent γ-transitions belong to the wanted nuclei ^{150}Eu or ^{152}Tb. In order to be sure of the isotopic identification only γ-transitions observed in γ-γ coincidence measurements have been put in the Tables 2 and 3.

The angular distributions of the γ-rays emitted during the ^{7}Li bombardment were measured by recording spectra taken at five angles (90°, 105°, 120°, 135° and 15 with the planar detector and five angles (270°, 288°, 305°, 320° and 335°) with 15% efficiency detector. The angular distributions of the γ-rays emitted during

the ^{11}B bombardment were measured by recording spectra taken at four angles (90°, 110°, 130° and 150°) with the planar detector and four angles (270°, 295°, 315° and 337°) with a 41% efficiency detector. The normalized peak areas were fitted with the angular distribution function :
$W(\theta) = A_o [1 + A_2 P_2 (\cos\theta) + A_4 P_4 (\cos\theta)]$. The information obtained from these γ-ray singles measurements is summarized in Tables 2 and 3 and fig.1 and 2 give examples of the singles γ-ray spectra observed.

In the γ-γ coincidence experiments four parameters were recorded for every coincidence event, the two γ-energies, the time between them and the time between one of them and the cyclotron radiofrequency. Two large volume Ge detectors of 15% and 41% efficiency were used and placed at ± 90° with respect to the beam direction. The results of the reduction to the two dimensional γ-γ coincidences are reported in the Tables 4 and 5 and some coincidence spectra are shown in Figs.3 and 4.

3. THE ^{152}Tb NUCLEUS

3.1. The level scheme of ^{152}Tb -

Before our investigations the γ-decay of the 4.2 mn high spin isomer (8^+) have been studied [10]. Considering the fact that this isomeric state is strongly fed in the $^{146}Nd(^{11}B,5n)$ reaction and that the levels below the isomeric state are not directly fed by prompt transitions we can conclude that measured γ-cascades end at the isomeric state.

In table 2 the relative intensities of the prompt transitions were transformed in per 1000 decays of the isomeric state. For this purpose we have used the value $I\gamma = 597$ previously measured for the intensity of the 283.3 KeV transition fed in the decay of the isomer [15].

The level scheme of ^{152}Tb populated by the (^{11}B, 5n) reaction is shown in Fig.5. It is based on the γ-γ coincidence measurements. Apart from the half life $T_{1/2}$ = 4 ns measured for the 1237.8 KeV level, timing measurements have shown that none of the included levels in the level scheme lives longer than ≲ 2 ns. We therefore consider E1, M1 and E2 as the only multipolarities contributing to the observed γ-decay. With this assumption and the results of angular distribution measurements and intensity balance considerations it is possible to determine the spin and parity assignments reported on Fig. 5.

In the Table 6 are reported the intensity balance of each level : the conversion electron intensities were computed assuming transitions of pure multipolarity. The table 6 shows that ≲ 86% of the total feeding of the isomeric state comes from discrete transitions, which seems reasonable.

- The 600.4 and 806.1 keV levels -

The angular distribution data of the 98.6, 205.7 and 304.3 KeV transitions show that the spin assignments correspond to the values I = 9 for the 600.4 KeV state and I = 10 for the 806.1 KeV state if it is assumed that the 98.6 KeV γ-ray feeds directly the 8^+ isomeric state. Moreover a positive parity is associated with these two levels from intensity balance considerations which are only compatible with a M1 multipolarity for the 98.6 and 205.7 KeV transitions.

The γ-rays of the two cascades feeding the 600.4 and 806.1 KeV levels have angular distributions compatible with stretched E2 transitions ; they de-excite very likely collective states based on the 9^+ and 10^+ levels.

- The isomeric state at 1237.8 KeV -

The half-life $T_{1/2}$ = 4.2 ± 0.2 ns was measured for the 431.7 and 710.7 keV transition

de-exciting the 1237.8 keV isomeric state (Fig.6). The anisotropies measured for the 98.6 and 205.7 keV transitions show that the near isotropic behaviour of the 431.7 KeV transition is not caused by the 4ns half-life. Then the value $A_2 = -0.03 \pm 0.02$ found is characteristic of a $\Delta I = 1$ transition with a L = 1, L = 2 multipole admixture. The absence of transitions to the 8^+ and 9^+ states strongly suggests a spin value I = 11 for the 1237.8 KeV isomeric level.

From our experimental data it is not possible to find the nature of the 431.7 Ke transition and the negative parity proposed is based on theoretical consideratio and will be discussed below. The M2-E1 mixing ratio extracted from angular distribution is $\delta = 0.15 \pm 0.05$ and the values found for the Weisskopf hindrance factors are : $F_W = 2 \times 10^6$ for the E1 transition and $F_W = 3.5 \pm 2.5$ for the M2 transition.

From γ-γ coincidence experiments it is evident that the 1237.8 keV state decays also on the 1212.5 KeV level. Unfortunately the transition energy deduced from the energy difference, $E\gamma = 25.3$ KeV is too low to be seen in our experiment.

On the 1237.8 KeV level is built a system of two groups of states which decay by γ transitions compatible with streched E2. Some of these states are connected up to 3126.7 KeV energy by $\Delta I = 1$ transitions with a very small L1, L2 admixture and we have then made the natural assumption that the considered levels make a unique collective structure built on the 1237.8 KeV level -

3.2.- Band structure in ^{152}Tb -

Zolnowski et al. [10] have proposed the deformed configuration $[532\ \frac{5}{2}]_p$ $[505\ \frac{11}{2}]_n$ for the 8^+ isomeric state in ^{152}Tb to explain the fast EC + β^+ decay to the 7^+ level in ^{152}Gd. This assignment is certainly not correct if we take

into account the moderately rotational character of the collective structures observed above the isomeric state. In fact the situation of the ^{152}Tb nucleus looks very much like those of the odd neutron N = 87 isotones : ^{149}Sm, ^{151}Gd and ^{153}Dy [16] where the collective states built on the neutron configurations $f\frac{7}{2}$, $h\frac{9}{2}$ and $i\frac{13}{2}$ have been observed. Then the three collective systems fed in ^{152}Tb correspond very likely to the same neutron orbitals coupled to the $h\frac{11}{2}$ proton shell (fig.5).

The configuration of the 8^+ isomeric state is now obvious :

$$[(f\,\tfrac{7}{2})^3\,;\,\tfrac{5}{2}]_n\,[h\,\tfrac{11}{2}]_p$$

and the fast transition to the 7^+ state in ^{152}Gd can be explained as :

$$\left\{[(f\,\tfrac{7}{2})^3\,;\,\tfrac{5}{2}]_n\,[h\,\tfrac{11}{2}]_p\right\}_{8^+} \rightarrow \left\{[(f\,\tfrac{7}{2})^3\,;\,\tfrac{5}{2}]_n\,[h\,\tfrac{9}{2}]_n\right\}_{7^+}$$

where the $h\,\frac{11}{2}$ proton is transformed in $h\,\frac{9}{2}$ neutron after β^+ + EC emission. A very low-lying $\frac{5}{2}$ state belonging to the $(f\,\frac{7}{2})^3$ neutron occurs systematically in the N = 87 isotones [17,18]. Its excitation energy decreases regularly with decreasing proton number and in ^{147}Nd it becomes the ground state [18]. The $\frac{7}{2}^-$ state of seniority ν = 1 is generally very close to the $\frac{5}{2}^-$ level and can be identified with the 9^+ state in ^{152}Tb at 600.4 KeV excitation energy when it is coupled with the $[h\,\frac{11}{2}]$ proton.

The ground state of the configuration $[h\,\frac{9}{2}]_n\,[h\,\frac{11}{2}]_p$ has been identified in ^{152}Tb at the excitation energy 806.1 keV. This assumption is in agreement with the fact that the energy difference (206 keV) between the 10^+ and 9^+ states in ^{152}Tb is close to the energy difference between the ground state of the $h\,\frac{9}{2}$ and $f\,\frac{7}{2}$ configuration in the odd neutron N = 87 isotones : 379 keV in ^{151}Gd and 296 keV in ^{153}Dy [16].

In ^{150}Tb and ^{154}Tb [8,2] the $[i\,\frac{13}{2}]_n\,[h\,\frac{11}{2}]_p$ system is very close to the yrast line and it is a natural assumption to assign the same configuration to

the well developped collective band built on the 1237.8 keV excitation energy in ^{152}Tb and strongly fed in the (^{11}B, 5n) reaction. In this case also the energy difference (770 keV) between the 12^+ and 9^+ states in ^{152}Tb is close to the energy difference between the ground state of the i $\frac{13}{2}$ and f $\frac{7}{2}$ configuration in the odd neutron N = 87 isotones : 852 keV in ^{151}Gd and 712 keV in ^{153}Dy [16]. This configuration assignment is also in agreement with the strong E1 and small M2 hindrance factor found for the 431.7 keV line which corresponds, to the transition :

$$[i\,\tfrac{13}{2}]_n\,[h\,\tfrac{11}{2}]_p \;\rightarrow\; [h\,\tfrac{9}{2}]_n\,[h\,\tfrac{11}{2}]_p$$

4. THE ^{150}Eu NUCLEUS

Prior to our investigations the decay of the 45 ns high-spin isomer (8^+) have been studied [9]. In the γ-γ coincidence experiments we have found strong intensity γ-cascades which end at the isomeric state. In contrast no substantial prompt γ-feeding of the well established levels below the isomeric state were observed. This absence of direct feeding is also apparent in Table 3 were the off-beam γ-intensities of the lines below the isomeric state measured by SORAMEL [9] are compared with the intensities following the ^{7}Li bombardment. In table 3 we have also transformed the relative intensity of the prompt transitions in per 1000 decays of the isomeric state. For this purpose we have deduced an absolute γ-intensity Iγ = 492 for the 247.9 KeV transition from the level scheme proposed by SORAMEL.

The level scheme of ^{150}Eu populated by the (^{7}Li, 5n) reaction is shown in Fig.7. It is based on the γ-γ coincidence measurements. Timing measurements have shown that none of the included levels in the level scheme lives longer than ≈ 2 ns and we have made the natural assumption that E1, M1 and E2 are the only multipolarities contributing to the observed γ-decay. The spin and parity assignments were deduced from angular distribution measurements, intensity balance considerations and from the direct comparison with ^{152}Tb nucleus. We have also deduced from our experiments that ≈ 95% of the total feeding of the isomeric state comes from the discrete transitions placed in the level scheme.

The transition placements in the ^{150}Eu level scheme is much more difficult than in the case of ^{152}Tb. The γ-γ coincidence experiments show that the 593 KeV transition is in fact a triplet of lines with about the same energy and that the 490 and 557 KeV are doublets. Moreover we suspect the presence of low energy transitions, not detected in singles or coincidence spectra,

which of course hamper considerably the construction of the level scheme ; these transitions are plotted in dot lines in Fig.7. The transition placement proposed in Fig.7 is probably the right solution, but other possibilities may exist.

Three collective bands are also observed in ^{150}Eu; from the same arguments developped in the former section they correspond very likely to the same configurations $[f\ \frac{7}{2}]_n\ [h\ \frac{11}{2}]_p$, $[h\ \frac{9}{2}]_n\ [h\ \frac{11}{2}]_p$ and $[i\ \frac{13}{2}]_n\ [h\ \frac{11}{2}]_p$ already observed in ^{152}Tb.

5. THEORETICAL DISCUSSION

With the completion of the present experiment it is possible to follow the coupling of the two particle configuration $[i\ \frac{13}{2}]_n\ [h\ \frac{11}{2}]_p$ with the core, from the spherical ^{150}Tb [8] to the deformed region (^{154}Tb [2], ^{152}Eu [1]). In Fig. 8 we have compared this configuration in three odd-odd Tb isotopes. At one end of the systematic, the ^{150}Tb "band" behaves like a multiplet of a two-particle configuration $[f\ \frac{7^2}{2}]_n$ with energy difference $\Delta E(I \rightarrow I-2)$ decreasing with increasing the spin I ; it is the general behaviour expected for a spherical nucleus. At the other end of the systematic, a rotational band strongly pertubed by Coriolis interaction was observed in ^{154}Tb. The ^{152}Tb nucleus is in an intermediate situation characteristic of a transitional nucleus.

In the three Tb isotopes two $\Delta I = 2$ bands coexist corresponding to the odd and even spins. In the deformed region we have shown [1,2] that this coexistence is predicted by the theory ; the most favoured bands correspond to the neutron placed in the $[i\ \frac{13}{2}\ ;\ \alpha = \frac{1}{2}]$ configuration while the proton may be placed either in the $[h\ \frac{11}{2}\ ;\ \alpha = -\frac{1}{2}]$ level giving $\alpha = 0$ (even spins) or the

$[h\frac{11}{2}; \alpha = -\frac{1}{2}]$ level giving $\alpha = 1$ (odd spins). The signature α is defined in the same way as in ref.[19]. The staggering between odd and even spin levels reflects mainly the alignment difference for the $[h\frac{11}{2}, \alpha = \pm\frac{1}{2}]$ levels.

In addition it has been found experimentally that at low rotational frequency the odd spin levels are more favoured than the even spin states and we have shown this unexpected effect can be explained by a triaxial shape for the $[i\frac{13}{2}]_n [h\frac{11}{2}]_p$ band ($\gamma \gtrsim 10°$ in ^{154}Tb) [2]. This γ-deformation seems to be correlated to the presence of the two strongly aligned particles rotating in a plan normal to the rotation axis.

In the spherical ^{150}Tb nucleus the 11^- state is also favoured compared to the 12^- level. It seems impossible to explain this effect as a consequence of the neutron-proton interaction which is more attractive for a parallel spin coupling and then favours the 12^- state. BRODA et al. [8] have explained the presence of this 11^- intruder state as the $[h\frac{11}{2}]_p [f\frac{7}{2}]_n$ configuration coupled to the 3^- octupole excitation. In reality this configuration is very likely mixed with the $[h\frac{11}{2}]_p [i\frac{13}{2}]_n$ configuration coupled to the spin value $I = 11$.

It seems then well established that the presence of a favoured 11^- state has a different origin in the spherical ^{150}Tb and in the deformed ^{154}Tb nucleus. In the transitional ^{152}Tb nucleus the same situation is observed but it is very difficult to decide in the absence of detailed calculations which is the prominent effect : a triaxial deformation or the admixture with the $(f\frac{7}{2}, h\frac{11}{2}, 3^-)$ configuration.

It is interesting, to study in a transitional nucleus like ^{152}Tb, the importance of the quadrupole deformation and possible deformation changes with rotation. For this purpose we have studied the moment of inertia and the transition probabilities in the ^{152}Tb nucleus.

The collective moment of inertia in ^{152}Tb and ^{150}Eu for the $[i\frac{13}{2}]_n\,[h\frac{11}{2}]_p$ band -

In these two nuclei the natural assumption was made that the full alignment i is reached : $i = 12\,\hbar$ for the even spin and $i = 11\,\hbar$ for the odd spin states. In ^{152}Tb, the collective moment of inertia, J_c, versus ω^2 plot (Fig.9 starts as in the case of a nearly spherical nucleus and reaches, for $\hbar\omega > 0.3$ MeV a rotational frequency region where it can be fitted by the Harris formula :

$$J_c = J_o + J_1\,\omega^2$$

with $J_o = 6.8$ MeV$^{-1}\,\hbar^2$ and $J_1 = 112$ MeV$^{-3}\,\hbar^4$. This J_1 value is comparable with the values found for the strongly aligned two quasiparticle-bands : S-band in even-even nuclei or $[i\frac{13}{2}]_n\,[h\frac{11}{2}]_p$ configuration in odd-odd nuclei [2]. The J_o value which can be correlated with the ε_2, ε_4 deformations [20] is compatible with a small quadrupole deformation : $\varepsilon_2 < 0.15$. In conclusion the behaviour of the collective moment of inertia strongly suggests that the deformation changes as a consequence of an increasing rotational frequency and reaches, some stable deformation for $\hbar\omega > 0.3$ MeV. Above the spin I = 19 a new increase of J_c is observed which could be correlated with the crossing by the $[(i\frac{13}{2})^3]_n\,[h\frac{11}{2}]_p$ configuration.

The behaviour of J_c in ^{150}Eu is more smooth. The J_1 value extracted from experimental data $J_1 \simeq 170$ MeV$^{-3}\,\hbar^4$ seems to be too large compared to the systematic and a part of the slope could be correlated with a smooth increase of the deformation in the rotational frequency range measured.

The transition rates in ^{152}Tb -

Very recently MARSHALEK [21] has derived approximate analytic formulas for E2 and M1 transition rates in the one quasiparticle decoupled bands. In this work we have extended this model to the $[i\frac{13}{2}]_n\,[h\frac{11}{2}]_p$ band by assuming

that the quasineutron plays a spectator role while the quasiproton is in the $[h\frac{11}{2}; \alpha = -\frac{1}{2}]$ level for even spin states and in the $[h\frac{11}{2}; \alpha = \frac{1}{2}]$ level for odd spin states. It is then easy to show that the transition probabilities in the considered band are the same as in the $[h\frac{11}{2}]_p$ band and the analytic formulas for one quasiparticle system can be applied in this case

The experimental B(M1)/B(E2) ratio plotted for ^{152}Tb and ^{154}Tb (Fig.10) shows a strong staggering caused by the signature splitting between even and odd spin states. Moreover, in the ^{152}Tb case, this ratio is compatible with zero for odd spin level, in the limit of the γ detection efficiency , which indicates a small value for the parameter C/A of the model [21] (A is related to the moment of inertia J by $A = \hbar^2/2J$ and C is characteristic of the $[h\frac{11}{2}]_p$ shell and the deformation). The theoretical ratio $X(I) = B(E2; I \to I-2)/B(M1; I \to I-1)$ and $Y(I) = B(E2; I \to I-1)/B(M1; I \to I-1)$ were then computed from the equations (61b), (66b) and (68b) of ref.[21] for C/A = 0 and C/A = 2. In addition the assumption was made that $q(\frac{11}{2})/Q_o \simeq 0$, $g_R = 0.35$ and the value $g_{\frac{11}{2}} = 1.11$ was extracted from the experimental magnetic moment of ^{149}Eu [15] ; the quantity q(J) is defined by equation (64) of ref.[21] and g_R and g_J are the collective and intrinsic gyromagnetic ratio. By comparison of the theoretical X(I) values with the corresponding experimental quantities it is then possible to extract the intrinsic quadrupole moment Q_o (Table 7). With the values found for Q_o it was also possible to extract the theoretical mixing ratio δ. A good agreement with experimental data is obtained in the case C/A = 2 (Table 7).

The most striking effect observed is the increase of the quadrupole moment Q_o ($\simeq$ 25%) between the 14^- and 18^- state in qualitative agreement with the behaviour of the moment of inertia and in conclusion there is strong indication of deformation change when the rotational frequency increases. The same effect has been experimentally and theoretically evidenced in the

odd and even-even N $\simeq$ 90 rare earth nuclei [22].

SUMMARY

The present (^{7}Li, 5n) and (^{11}B, 5n) experiments have established the previously unknown high-spin states in the two odd-odd nuclei ^{150}Eu and ^{152}Tb. Three decoupled bands have been evidenced in this work, corresponding to the $[f\,\frac{7}{2}]_n\,[h\,\frac{11}{2}]_p$, $[h\,\frac{9}{2}]_n\,[h\,\frac{11}{2}]_p$ and $[i\,\frac{13}{2}]_n\,[h\,\frac{11}{2}]_p$ configurations. The latter one, strongly fed, is well developped and improves our knowledge of the $[i\,\frac{13}{2}]_n\,[h\,\frac{11}{2}]_p$ system between the spherical and deformed region.

The analysis of the moment of inertia and transition probabilities strongly suggests an increase of the deformation with the angular momentum. Another striking effect evidenced (in this paper) is that the odd spin levels are more favoured than the even spin states in the $[i\,\frac{13}{2}]_n\,[h\,\frac{11}{2}]_p$ configuration. In absence of detailed calculations it is difficult to assign this effect to the occurence of a triaxial shape in ^{150}Eu and ^{152}Tb or to an admixture with the $[f\,\frac{7}{2},\ h\,\frac{11}{2},\ 3^-]$ octupole configuration.

REFERENCES

1. PINSTON J.A., BENGTSSON R., MONNAND E., SCHUSSLER F. and BARNEOUD D. :
Nucl. Phys. A361, 464 (1981).

2. BENGTSSON R., , PINSTON J.A., BARNEOUD D., MONNAND E. and SCHUSSLER F. :
Nucl. Phys. A389, 158 (1982).

3. LØVHØIDEN G. :
The 3rd Bergen workshop in Nuclear Physics, Nov. 25-26 (1980) and
Phys. Scripta 25, 459 (1982).

4. RIZK N. and BOUTET J. :
J. de Phys. Lett. 37, 197 (1976).

5. LEIGH J.R., STEPHENS F.S. and DIAMOND R.M. :
Phys. Lett. 37, 197 (1976).

6. DRISSI S., ANDRE S., GENEVEY J., BARCI V., GIZON A., PINSTON J.A.,
JABSTRZEBSKI J., KOSSAKOWSKI R. and PREIBISZ Z. :
Z. Phys. A. - Atoms and Nuclei : 304, 293 (1982).

7. BRODA R., BEHAR M., KLEINHEINZ P. , DALY P.J. and BLOMQVIST J. :
Z. Phys. A. - Atoms and Nuclei : 293, 135 (1979).

8. BRODA R., OGAWA N., KLEINHEINZ P., SCHELINE R.K. and RICHTER L. :
KFA Jülich Annual Report, 29 (1978).

9. SORAMEL F., STYCZEN J., ERCAN A., PROKOFJEV P. and KLEINHEINZ P. :
KFA Jülich Annual Report, 55 (1981).

SORAMEL F. : Thesis, Padova (1981).

10. ZOLNOWSKI D.R., HUGHES M.B., HUNT J. and SUGI CHARA T.T. :
Phys. Rev. C21, 2556 (1980).

11. LEIGH J.R., DRACOULIS G.D., SLOCOMBE N.G. and NEWTON J.O. :
J. Phys G : Nucl. Phys. 3, 519 (1977).

12. KEMNITZ P., FUNKE L., STARY F., WILL E., WINTER G., ELFSTRÖM S., HJORTH S.A.,
and LINDBLAD Th. : Nucl. Phys. A311, 11 (1978).

13. WINTER G., DÖRING J., FUNKE L., KEMNITZ P., WILL E., ELFSTRÖM S., ILIORTH S.A., JOHNSON A. and LINBLAD Th. :
Nucl. Phys. A299, 285 (1978).

14. Table of Isotopes, ed. LEDERER C.M. and SHIRLEY V.S. :
(Willey, New York, 1978).

15. BAGLI C.M. :
Nuclear Data Sheets 30, 1 (1980).

16. KLEINHEINZ P., STEFANINI A.M., MAIER M.R., SHELINE R.K., DIAMOND R.H. and STEPHENS F.S. :
Nucl. Phys. A 283, 189 (1977).

17. ROUSSILLE R., PINSTON J.A., BRAUMANDL F., JEUCH P., LARYSZ J., MAMPE W. and SCHREKENBACH K. :
Nucl. Phys. A258, 257 (1976).

18. ROUSSILLE R., PINSTON J.A., BÖRNER H., KOCH H.R., HECK D. :
Nucl. Phys. A246, 380 (1975).

19. BENGTSSON R. and FRAUENDORF S. :
Nucl. Phys. A327, 139 (1979).

20. BENGTSSON R. :
Intern. Conf. on Nuclear Behaviour at High Angular Momentum,
J. de Phys. C10, 79 (1980).

21. MARSHALEK E.R. :
Phys. Rev. C26, 1678 (1982).

22. BENGTSSON R., MAY F.R. and PINSTON J.A. :
XX Intern. Winter meeting on Nucl. Phys. - Bormio, 144 (1982).

FIGURE CAPTIONS

1. Gamma ray singles spectrum obtained from bombardment of $^{146}Nd_2O_3$ with 66 MeV ^{11}B-particles at 90° to the beam direction.

2. Gamma ray singles spectrum obtained from bombardment of $^{148}Nd_2O_3$ with 50 MeV ^{7}Li-particles at 90° to the beam direction.

3. Selected γ-γ coincidence spectra in ^{152}Tb.

4. Selected γ-γ coincidence spectra in ^{150}Eu.

5. Level scheme of ^{152}Tb. The widths of the arrows indicate the transition intensities. The 25.3 KeV γ-ray was not observed directly but deduced from the energy difference between the $11^{(-)}$ (1237.8 KeV and (9^-) (1212.5 KeV) states.

6. Decay of the 431.7 and 710.7 KeV transitions in ^{152}Tb.

7. Level scheme of ^{150}Eu. A line appearing twice or more in the level scheme is indicated by a cross.

8. a)- taken from [ref.8]
   b)- taken from [ref.2]
   Evolution of the $[i\frac{13}{2}]_n$ $[h\frac{11}{2}]_p$ band in three Tb isotopes between the spherical (^{150}Tb) and deformed region (^{154}Tb). The ε_2 value reported for ^{152}Tb corresponds to the mean value of the computed-quadrupole deformations (see Table

9. The collective moment of inertia J_{coll} plotted versus the squared rotational frequency in ^{150}Eu, ^{152}Tb and ^{154}Tb (ref.2). The full alignment was assumed in the case of ^{150}Eu and ^{152}Tb.

10. The experimental ratio (B(M1 ; I → I-1)/B(E2 ; I → I-2) plotted versus the angular momentum I in ^{152}Tb and ^{154}Tb (ref.2). A strong perturbation effect correlated to the signature splitting is observed.

Table 1

Relative cross-sections of the main reaction channels with ^{7}Li(50 MeV) and ^{11}B(66 MeV) beams.

Table 2

Gamma rays in ^{152}Tb observed in singles γ-ray spectra from ^{146}Nd (^{11}B,5n) reaction. The intensity normalization corresponds to 1000 decays of the 4.2 mn isomeric state.

Table 3

Gamma rays in ^{150}Eu observed in singles γ-ray spectra from ^{148}Nd (^{7}Li,5n) reaction. The intensity normalization corresponds to 1000 decays of the 45 ns isomeric state. In the table are also reported the off-beam γ-ray intensities measured by SORAMEL (ref. 9) in (p,3n) reaction.

Table 4

Qualitative summary of coincidence results in ^{152}Tb.

Table 5

Qualitative summary of coincidence results in ^{150}Eu.

Table 6

Intensity balances on the ^{152}Tb levels.

Table 7

Quadrupole moment Qo and quadrupole deformation ε_2 of ^{152}Tb extracted by comparison of the experimental ratio B(E2 ; I → I-2)/B(M1 ; I → I-1) with the theoretical analytic formulas of MARSHALEK [21] as a function of the parameter C/A. Comparison of the theoretical and experimental mixing ratio δ as a function of the parameter C/A.

Table 1

Evaporation particles	Incident ion and target	
	$^{7}Li+^{148}Nd$	$^{11}B+^{146}Nd$
4n	16	60
5n	100[d]	100[d]
6n	20	4
p,4n	≤16	≤30
α,3n	[b]	13

d) normalization

b) The final nucleus ^{148}Pm is unknown

Table 2

E_γ (keV)	Intensity	Ang. dist. Coeff. A_2/A_0	Ang. dist. Coeff. A_4/A_0	Mixing ratio	Assignments $I_i^\pi \rightarrow I_f^\pi$
98.55	204	-0.21(03)	-0.06(05)	-0.05±0.10	$9^+ \rightarrow 8^+$
123.78	22	-0.18(20)	-0.16(21)		
132.44	56	-0.15(04)	-0.08(08)	0.05±0.03	$12^{(-)} \rightarrow 11^{(-)}$
205.74	396	-0.16(02)	-0.06(06)	0.01±0.05	$10^+ \rightarrow 9^+$
208.11	68	-0.20(05)	-0.03(07)	0.01±0.05	$14^{(-)} \rightarrow 13^{(-)}$
229.93	66	-0.12(08)	-0.13(11)	0.06±0.06	$16^{(-)} \rightarrow 15^{(-)}$
237.1	30				$18^{(-)} \rightarrow 17^{(-)}$
304.33	51	0.19(10)	-0.05(16)		$10^+ \rightarrow 8^+$
328.8	23	-0.40(19)	0.45(19)		
352.9	72				
391.5	26	0.08(18)	0.12(26)		
431.66	408	-0.03(02)	-0.02(03)	0.15±0.05	$11^{(-)} \rightarrow 10^+$
474.37	393	0.29(02)	-0.01(05)		$13^{(-)} \rightarrow 11^{(-)}$
538.5	81	0.40(12)	-0.08(22)		$14^+ \rightarrow 12^+$
545.1	176	0.35(08)	-0.02(14)		$12^+ \rightarrow 10^+$
550.1	95	0.31(06)	-0.03(10)		$14^{(-)} \rightarrow 12^{(-)}$
557.3	273	0.28(05)	-0.04(09)		$15^{(-)} \rightarrow 13^{(-)}$
579.3	114	0.31(07)	-0.05(12)		$16^{(-)} \rightarrow 14^{(-)}$
592.6	59	-0.01(06)	0.07(09)		
612.1	52	0.16(13)	-0.04(19)		$(9^-) \rightarrow 9^+$
620.0	109	0.35(12)	0.01(17)		$17^{(-)} \rightarrow 15^{(-)}$
627.4	69	0.27(15)	0.13(18)		$18^{(-)} \rightarrow 16^{(-)}$
629.8	79	0.34(12)	0.00(17)		$11^+ \rightarrow 9^+$
657.7	39				$13^+ \rightarrow 11^+$
706.7	26	0.42(18			$19^{(-)} \rightarrow 17^{(-)}$
710.7	127	-0.08(11)	-0.02(16)		$(9^-) \rightarrow 8^+$
718.6	38	0.30(15)	0.02(22)		$20^{(-)} \rightarrow 18^{(-)}$
740.1	22	0.37(19)	-0.31(30)		
754.0	17	0.30(08)	-0.02(14)		$21^{(-)} \rightarrow 19^{(-)}$
800.9	33	0.24(18)	-0.07(28)		$16^+ \rightarrow 14^+$

Table 3

E (keV)	Intensity (^{11}B,5n)	Intensity (p,3n)	Ang. dist. coeff. A_2/A_0	Ang. dist. coeff. A_4/A_0	Mixing ratio δ	Assignments $I_i^\pi \rightarrow I_f^\pi$
107.74	44		-0.026(05)	-0.10(07)		
129.38	270		-0.29(03)	-0.04(03)	-0.18 ± 0.10	9^+ 8^+
163.66	297		-0.23(02)	0.01(04)	-0.04 ± 0.05	(11^-) 10^+
171.38	46	44				
189.96	150		0.06(02)	0.01(03)		10^+ 8^+
190.34	375	379				
197.1						
222.11	27	29	-0.15(05)	-0.05(08)		
226.90	81	47	0.09(09)	0.03(11)		
240.22	81		-0.02(10)	-0.25(12)		
247.92	492	492	-0.02(03)	0.04(04)		
314.16	536	527	0.08(03)	0.01(04)		
341.87	26		-0.07(07)	-0.07(10)		
371.70	319	327	0.11(04)	0.03(06)		
381.67	29		-0.12(05)	0.02(08)		
387.30	35		-0.06(05)	0.13(08)		
415.10	234		0.34(06)	-0.06(08)		(14^-) (12^-)
424.81	65		0.42(07)	-0.33(11)		
428.99	83		0.38(07)	-0.10(11)		10_2^+ 10_1^+
440.68	43		0.23(15)			
456.93	254		0.38(06)	-0.22(08)		12^+ 10_1^+
465.97	158		0.35(12)	-0.07(15)		
489.69	106		-0.16(5)			10_2^+ 9^+
.9	61					
556.7	258		0.26(06)	0.00(08)		(16^-) (14^-)
592.8	251					$11^{(-)}$ 10^+
						(14^+) 12^+
						(15^-) $13^{(-)}$
619.0	222		0.38(06)	-0.02(08)		10_2^+ 8^+
622.5	36		0.30(10)			
642.9	59		0.24(06)	0.02(08)		(18^-) (16^-)
666.9	34		0.26(10)			(17^-) (15^-)
718.4	38		0.16(15)			(20^-) (18^-)

Table 4

Gate Transition	Coincident transitions
98.6	132, 206, 208, 230, 432, 474, 539, 543, 550, 579, 612, 620, 627, 630
123.8	98, 206, (208), (230), 237, 432, 474, 557, 627
152.3	98, 124, 206, 304, 432, 550, 579, 627, 771
205.7	98, 124, 132, 173, 191, 208, 230, 237, 329, 392, 432, 474, 539, 543, 550, 557, 579, 620, 627, (707), (719), 740, 801
208.1	98, 124, 206, 304, 353, 432, 474, 579, (593), 620, 627, 711, (719), 740
229.9	98, 124, (353), 432, 474, 557, (593), 627
237.1	(98), 124, 206, 432, 474, 557, 593, 620, 710
304.3	132, 208, 432, 474
328.8	206, 432, 474, 557, 620
391.8	206, 432, 474, 557
431.7	98, 124, 132, 191, 206, 208, 230, 237, 304, 392, 474, 550, 557, 579, 620, 627, 740
474.4	98, 124, 191, 206, 208, 230, 237, 304, (329), (353), 392, 557, 579, (612), 620, 627, 711, (719)
538.5	98, 206, 304, 543, 801
543.1	98, 206, 304, 539, 801
550.1	98, 132, 206, 432, 579, 627, 711, 740
557.3	98, (124), 206, 230, 237, 304, 353, 392, 432, 474, 612, 620, 627, 707, 711, 719
579.3	98, (124), 132, 206, 209, 353, 432, 474, 550, 627, 711
592.6	(206), 230, (237), 474, 627
620.0	98, 206, 237, 329, 432, 474, 558, 707, 711, 754
627.4	98, 124, 152, 206, 208, 230, 304, 432, 474, 550, (557), 579, 593 711
629.8	98, 658
706.7	206, 208, 432, 474, 557, 620
710.7	132, 208, 230, 474, 550, 557, 579, (593), 620, 627, 707
718.6	98, 206, (230), 237, 432, 474
800.9	98, 206, 539, 543

Table 5

Gate Transition	Coincident transitions
108[d?]	129, 164, 190, 227, 248, 314, 342, 372, 405, 466, 557, 593, 619, 667
129	108, 164, 171, 190, 194, 197, 222, 240, 248, 251, 314, 372, 415, 425, 429, 440, 457, 466, 490, 557, 563, 593, 622, 800
164	108, 129, 141, 171, 190, 197, 227, 248, 256, 314, 319, 342 346, 368, 372, 382, 387, 405, 415, (418), 425, 429, 466, 490, 518, 539, 557, 562, 593, 619, 643, 667, 680, 704
169 + 170 + 171	108, 129, (164), 190, 227, 248, 270, 345, 466, 511, 557, 619, 658
190[d]	108, 129, 164, 171, 190, 222, 227, 240, 248, 314, 372, 382, 387, 415, 425, 429, 457, 466, 490, 557, 593, 619, 667, 705, 800, 871
197	129, 190, 248, 314, 457, 593, 800
227	(108), 129, 164, 171, 190, (238), 415, 557, 593
248	108, 129, 164, 171, 190, 314, (318), 415, 457, 466, 557, 593, 619
314	108, 129, 164, 190, (197), 248, 415, 457, 466, 557, 593, 619, 643
342	(108), 129, 164, 415, (452), 511, 557, 619
372	129, 164, 190, (197), 415, 457, 466, 557, 593, 619
382	(108), 129, 164, 190, 372, 415, 429, 518, 619, 681
387	108, 164, 190, 529, 425, 466, 593
415	129, (140), 164, 190, 227, 248, 314, 342, 372, 382, 429, 490, 557, 593, 619, 622, 718
425	(108), 129, 164, 190, 197, 222, 248, 314, 342, 372, 388, 440, 457, 466, 557, 593, 619
429	129, 164, 190, 248, 261, 286, 306, 314, 415, 466, 490, 522, 557, 593, 622, 628, 679
457	129, 171, 190, 197, 248, 268, 306, 314, 372, 425, 441, 557, 593, 800, 875
466	108, 129, 164, 190, 227, 248, 314, 387, 490, 557, 593, 619, 666
490[d]	129, 164, 171, (190), 248, 302, 306, 314, (344), 372, 384, 415, 451, 462, 466, 490, 517, 557, 593, 622
518	164, 381, 415, 429, 457, 490
557	108, 129, 164, 190, 248, 311, 314, 342, 372, 395, 405, 415, 425, 457, 466, 479, 490, 564, 593, 619, 643, (666)
592	164, 466, 666
593	190, 457, 800

Table 5 (follow)

592 + 593	108, 129, 164, 190, 197, 248, 314, 372, 387, 415, 425 441, 457, 466, 490, 557, 593, 619, 666, 800
619	(108), 164, 190, 248, 314, 342, 372, 388, 415, 466, 557, 593, 666
622	129, 557, 593
643	129, 164, 190, 415, 557, (619)
667	129, 164, 190, 214, 248, 314, 372, 466, 490, 593
800	129, 190, 197, (222), 248, 457, 593, (615), (641)

d) doublet

Table 6

Excitation energy keV	Feeding intensity	Deexciting intensity
501.8	861	1000
600.4	643	680
806.1	584	566
1230.1	39	79
1237.8	505	≥ 587
1349.2	81	176
1370.2	95	112
1712.1	360	393
1887.6	33	81
1920.3	136	182
2269.4	215	273
2499.5	69	194
2889.4	62	109
3126.7	38	105
3596.1	17	26

Table 7

I	$Q_0 e^2$ fm^2 and (ε_2)				δ		
	C/A = 0		C/A = 2		C/A = 0	C/A = 2	Exp.
12					∞	0.043	0.05 ± 0.03
14	186	(0.09)	204	(0.10)	0.12	0.046	0.01 ± 0.05
16	227	(0.11)	244	(0.11)	0.08	0.046	0.06 ± 0.06
18	239	(0.11)	251	(0.12)			

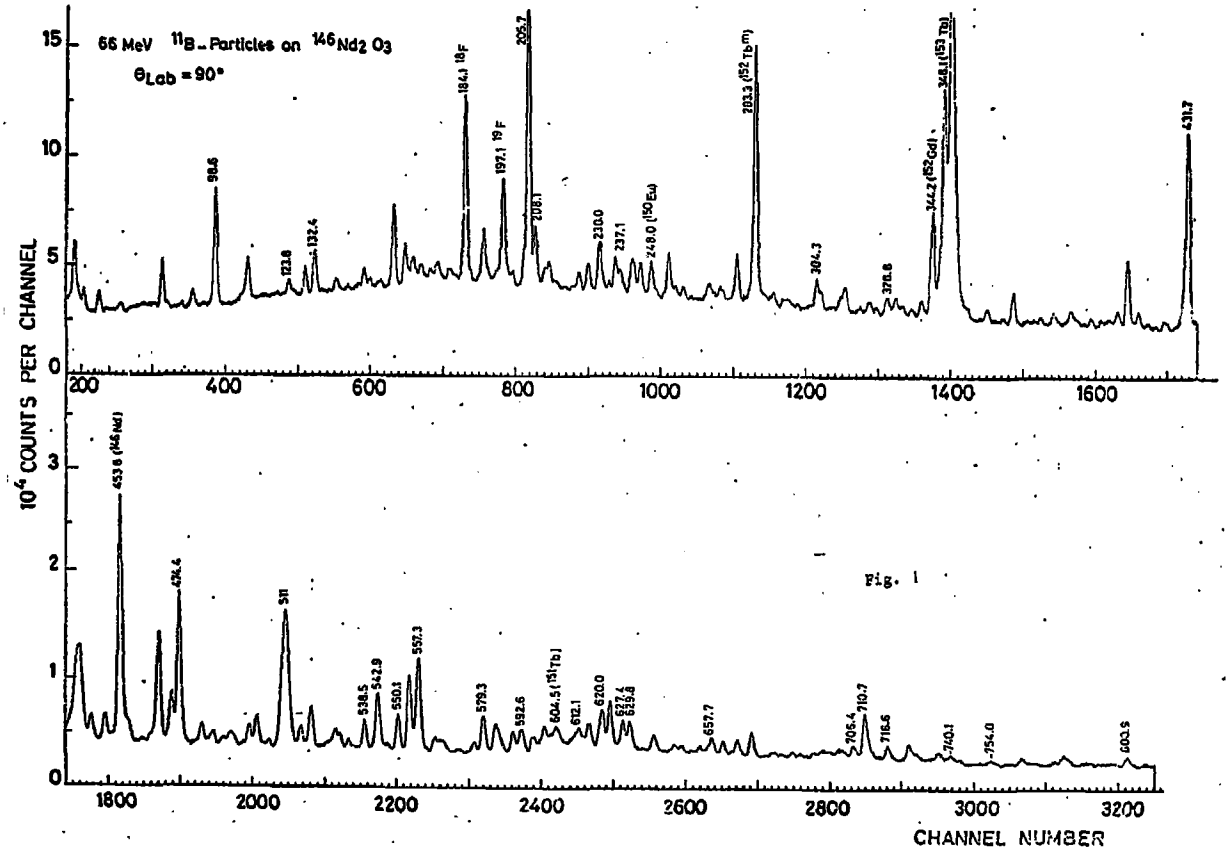
66 MeV ^{11}B - Particles on $^{146}Nd_2O_3$
$\theta_{Lab} = 90°$
10^4 COUNTS PER CHANNEL
CHANNEL NUMBER
98.6
123.8
132.4
184.1 ^{18}F
197.1 ^{19}F
205.2
208.1
230.0
237.1
248.0 (^{150}Eu)
283.3 ($^{152}Tb^m$)
304.3
378.8
344.2 (^{152}Gd)
348.1 (^{153}Tb)
431.7
453.8 (^{146}Nd)
496.4
511
538.5
542.9
550.1
557.3
579.3
592.6
604.5 (^{151}Tb)
612.1
620.0
627.4
635.8
657.7
705.4
710.7
716.6
740.1
754.0
803.5

Fig. 1

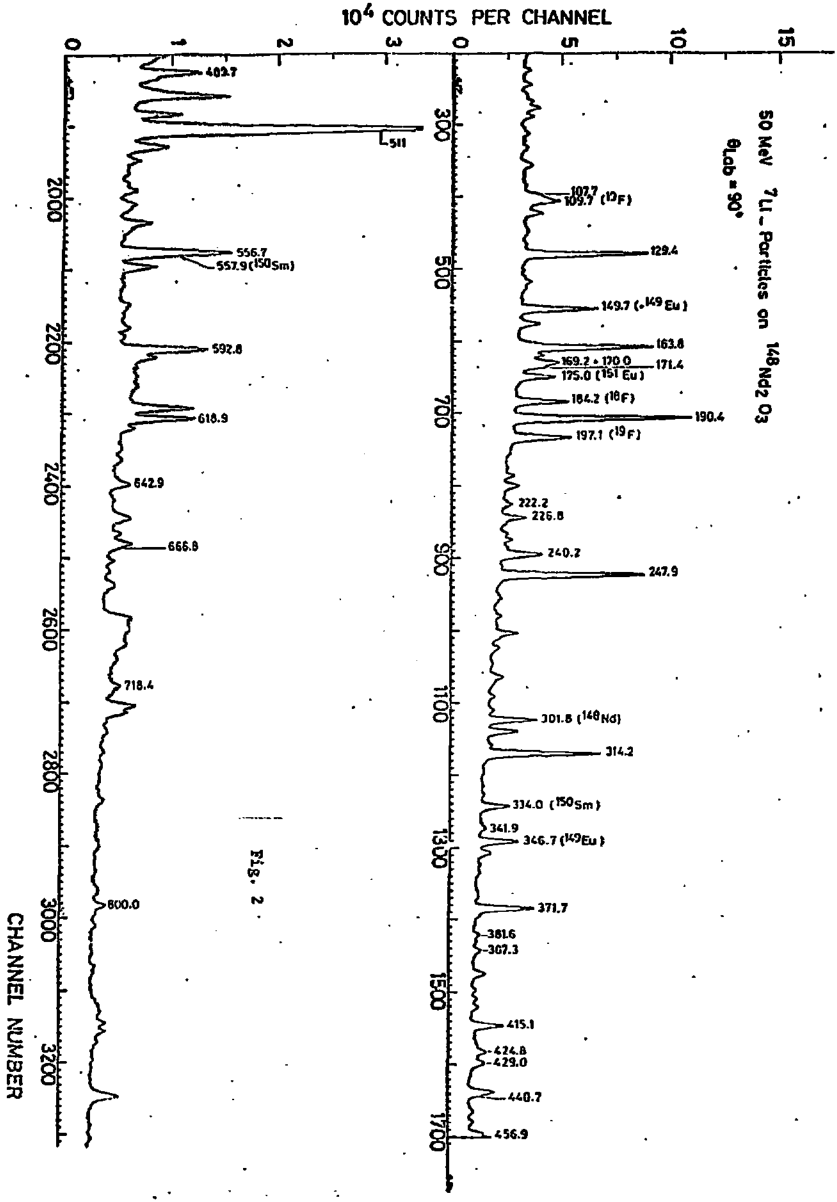

10^4 COUNTS PER CHANNEL
0
1
2
3
0
5
10
15
50 MeV ^{7}Li – Particles on ^{148}Nd$_2$O$_3$
$\theta_{Lab} = 90°$
300
500
700
900
1100
1300
1500
1700
2000
2200
2400
2600
2800
3000
3200
CHANNEL NUMBER
107.7
109.7 (^{19}F)
129.4
149.7 (+^{149}Eu)
163.8
169.2 + 170.0
171.4
175.0 (^{151}Eu)
184.2 (^{18}F)
190.4
197.1 (^{19}F)
222.2
226.8
240.2
247.9
301.8 (^{148}Nd)
314.2
334.0 (^{150}Sm)
341.9
346.7 (^{149}Eu)
371.7
381.6
387.3
415.1
424.8
429.0
440.7
456.9
482.7
511
556.7
557.9 (^{150}Sm)
592.8
618.9
642.9
666.8
718.4
800.0

Fig. 2

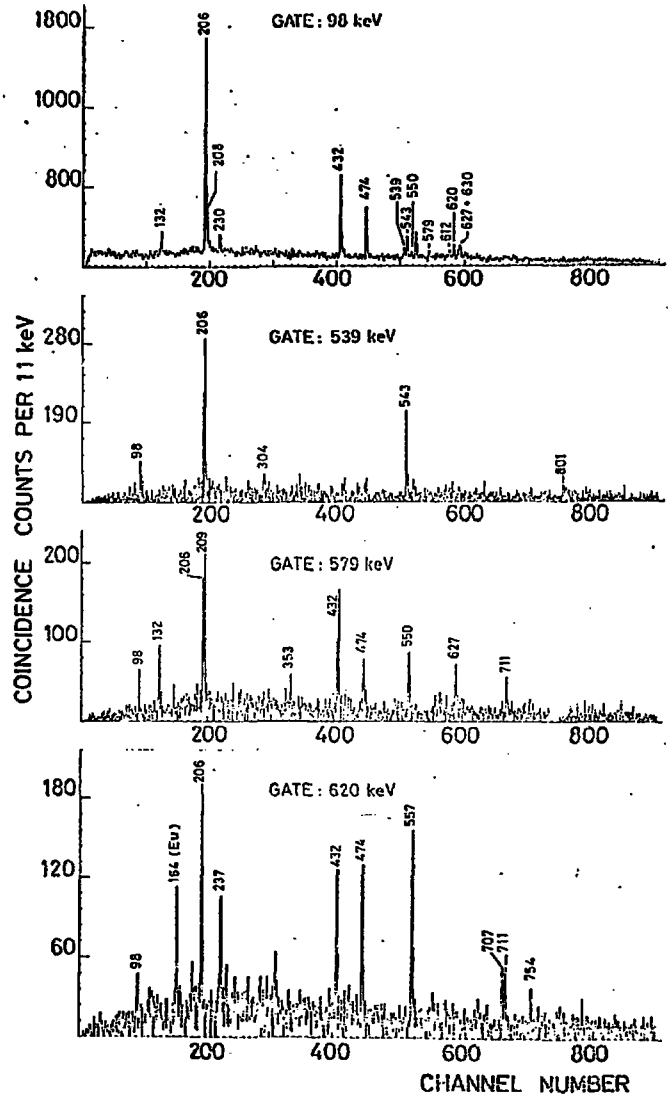
GATE: 98 keV
GATE: 539 keV
GATE: 579 keV
GATE: 620 keV
COINCIDENCE COUNTS PER 11 keV
CHANNEL NUMBER

Fig. 3

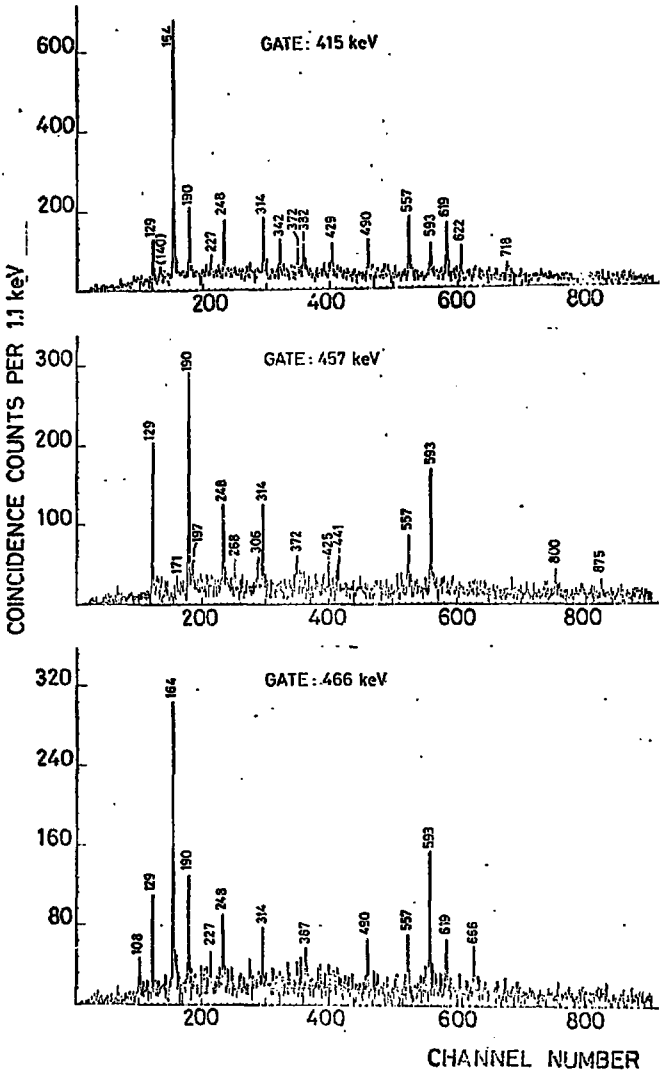
GATE: 415 keV
GATE: 457 keV
GATE: 466 keV
COINCIDENCE COUNTS PER 1.1 keV
CHANNEL NUMBER

Fig. 4

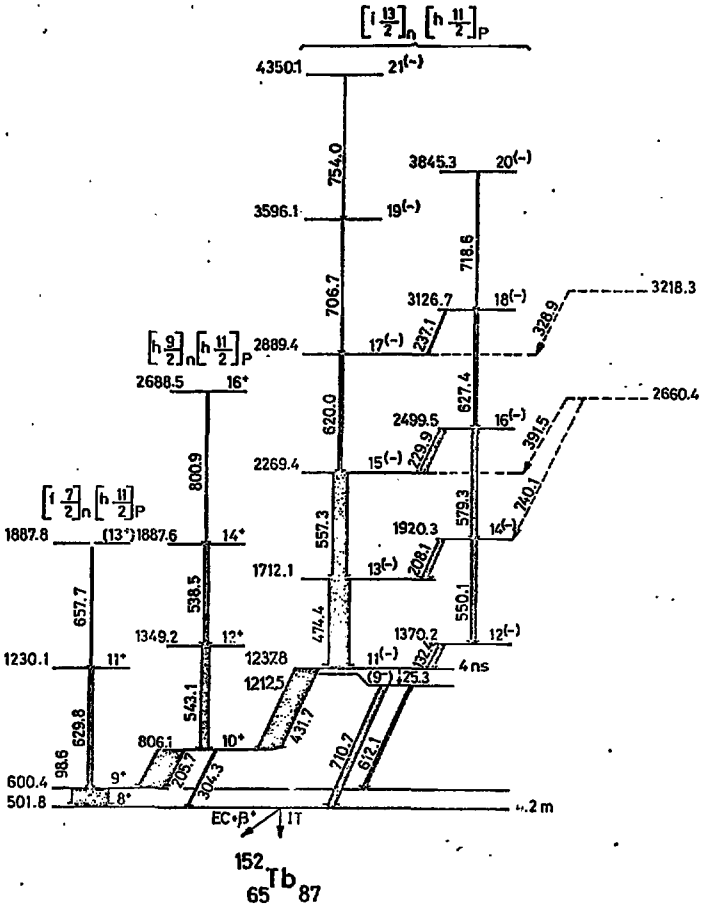
$[i\frac{13}{2}]_n[h\frac{11}{2}]_P$
4350.1
21(-)
754.0
3845.3
20(-)
3596.1
19(-)
718.6
706.7
3126.7
18(-)
3218.3
328.9
237.1
$[h\frac{9}{2}]_n[h\frac{11}{2}]_P$
2889.4
17(-)
2688.5
16+
620.0
627.4
2499.5
16(-)
2660.4
391.5
229.9
2269.4
15(-)
800.9
740.1
$[i\frac{7}{2}]_n[h\frac{11}{2}]_P$
579.3
1887.8
(13+)
1887.6
14+
1920.3
14(-)
557.3
208.1
1712.1
13(-)
657.7
538.5
550.1
474.4
1349.2
12+
1370.2
12(-)
1230.1
11+
12328
11(-)
32.2
4 ns
12125
(9-)
125.3
543.1
629.8
806.1
10+
431.7
710.7
612.1
98.6
600.4
9+
205.7
304.3
501.8
8+
EC+β+
IT
2 m
152 65 Tb 87

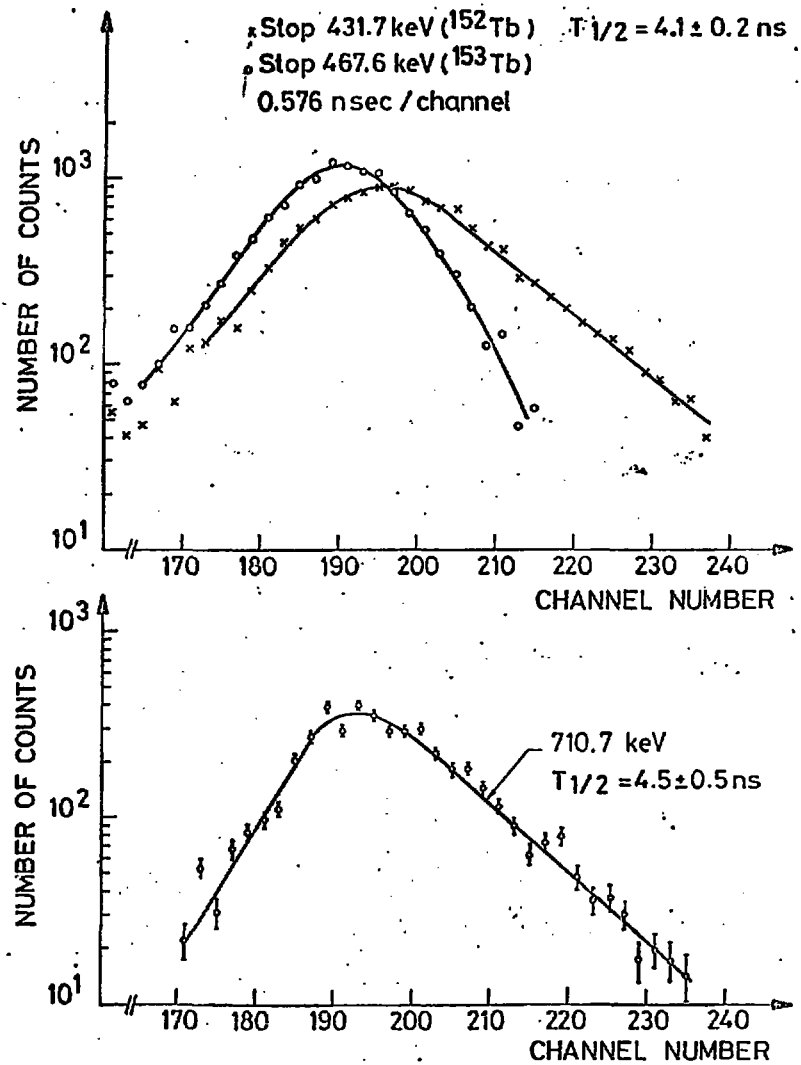
Stop 431.7 keV (^{152}Tb) T 1/2 = 4.1 ± 0.2 ns
Stop 467.6 keV (^{153}Tb)
0.576 n sec / channel
NUMBER OF COUNTS
10^3
10^2
10^1
170 180 190 200 210 220 230 240
CHANNEL NUMBER
710.7 keV
T1/2 = 4.5±0.5 ns
NUMBER OF COUNTS
10^3
10^2
10^1
170 180 190 200 210 220 230 240
CHANNEL NUMBER

Fig. 6

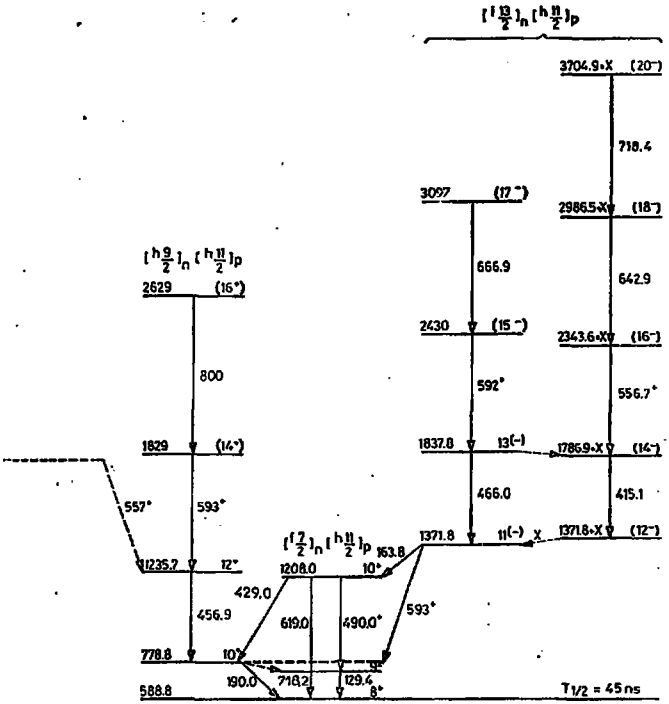
$[f_{\frac{13}{2}}]_n[h_{\frac{11}{2}}]_p$
3704.9+X (20⁻)
718.4
3097 (17⁻)
2986.5+X (18⁻)
666.9
642.9
2430 (15⁻)
2343.6+X (16⁻)
592*
556.7*
1837.8 13(-)
1786.9+X (14⁻)
466.0
415.1
1371.8 11(-) X
1371.8+X (12⁻)
$[h_{\frac{9}{2}}]_n[h_{\frac{11}{2}}]_p$
2629 (16⁺)
800
1829 (14⁺)
557*
593*
1235.7 12⁺
$[f_{\frac{7}{2}}]_n[h_{\frac{11}{2}}]_p$
163.8
1208.0 10⁺
429.0
456.9
619.0
490.0*
593*
778.8 10⁺
190.0
718.2
129.4
588.8 8⁺
$T_{1/2}$ = 45 ns

$^{150}_{63}Eu_{87}$

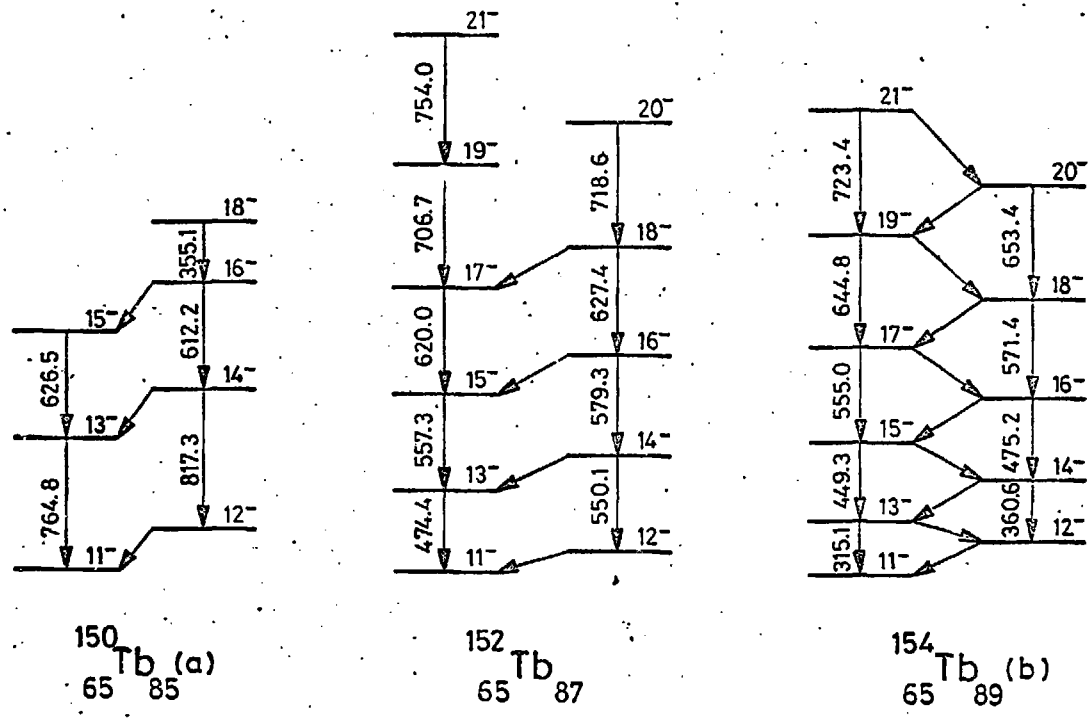
ε2 ≈ 0
ε2 ≈ 0.11
ε2 ≈ 0.16 γ ≈ 10°
18⁻
16⁻
15⁻
14⁻
13⁻
12⁻
11⁻
355.1
612.2
626.5
817.3
764.8
21⁻
20⁻
19⁻
18⁻
17⁻
16⁻
15⁻
14⁻
13⁻
12⁻
11⁻
754.0
706.7
620.0
557.3
474.4
718.6
627.4
579.3
550.1
21⁻
20⁻
19⁻
18⁻
17⁻
16⁻
15⁻
14⁻
13⁻
12⁻
11⁻
723.4
644.8
555.0
449.3
315.1
653.4
571.4
475.2
360.6
150 65 Tb 85 (a)
152 65 Tb 87
154 65 Tb 89 (b)

Fig. 6

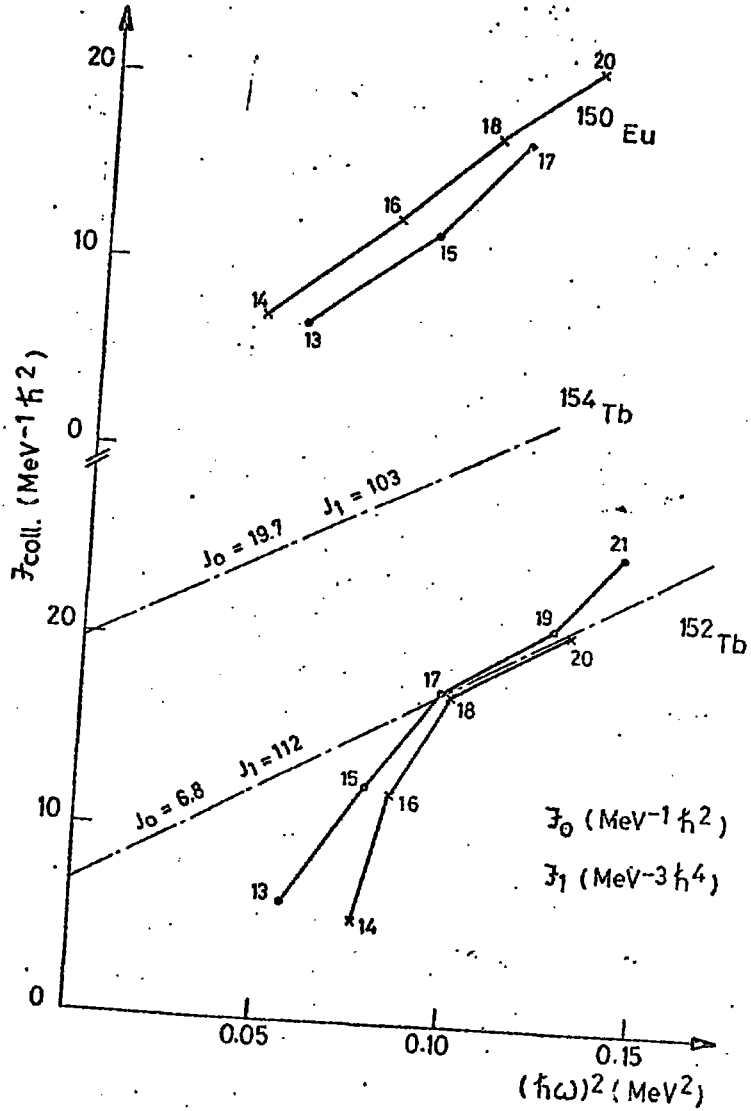
20
10
0
20
10
0
$\mathcal{J}_{coll.}$ (MeV$^{-1}\hbar^2$)
^{150}Eu
^{154}Tb
^{152}Tb
$J_0 = 19.7$
$J_1 = 103$
$J_0 = 6.8$
$J_1 = 112$
$\mathcal{J}_0$ (MeV$^{-1}\hbar^2$)
$\mathcal{J}_1$ (MeV$^{-3}\hbar^4$)
0.05
0.10
0.15
$(\hbar\omega)^2$ (MeV^2)

FIG. 9

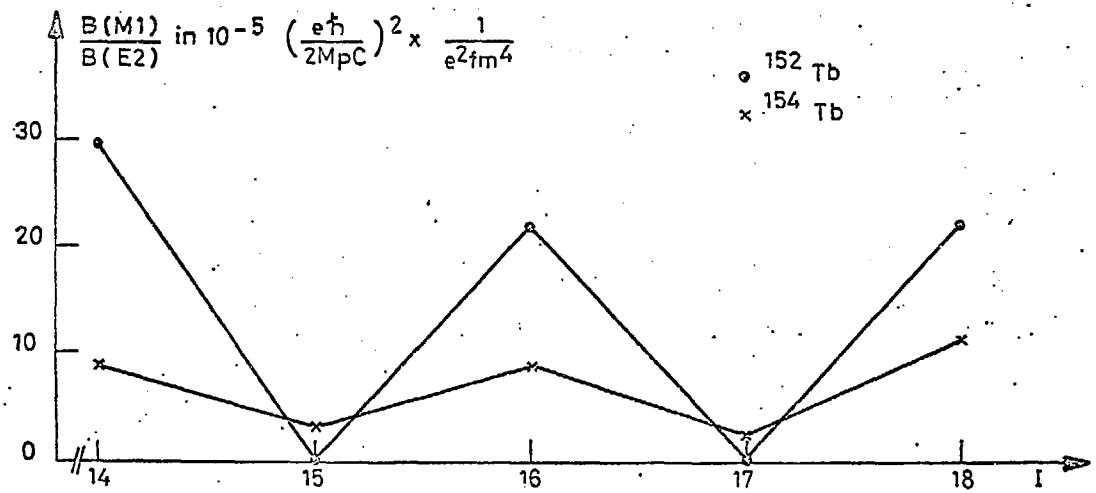
B(M1)/B(E2) in 10-5 (eħ/2MpC)2 x 1/e2fm4
152 Tb
154 Tb
30
20
10
0
14
15
16
17
18
I

Fig. 10